Am J Transl Res 2023;15(3):1862-1870
www.ajtr.org /ISSN:1943-8141/AJTR0145613

Original Article

Dynamic contrast-enhanced magnetic resonance imaging in epithelial ovarian tumor categorization: comparison with apparent diffusion coefficient histogram analysis and the tumor cell proliferation marker

Qing Zhou[1*], Jun Jin[2*], Yingfang Wang[1], Yida Wang[3], Tianping Wang[1], He Zhang[1], Yuantao Liu[4]

[1]*Department of Radiology, Obstetrics and Gynecology Hospital of Fudan University, Shanghai, P. R. China;*
[2]*Department of Pathology, Obstetrics and Gynecology Hospital of Fudan University, Shanghai, P. R. China;*
[3]*Shanghai Key Laboratory of Magnetic Resonance, East China Normal University, Shanghai, P. R. China;*
[4]*Department of Gynecology, Obstetrics and Gynecology Hospital of Fudan University, Shanghai, P. R. China.* [*]*Equal contributors.*

Received July 28, 2022; Accepted February 2, 2023; Epub March 15, 2023; Published March 30, 2023

Abstract: Objective: To compare the capability of dynamic contrast-enhanced (DCE) magnetic resonance imaging (MRI) and apparent diffusion coefficient (ADC) histogram analysis in epithelial ovarian tumor categorization. Methods: We retrospectively recruited 52 patients with pathologically proven ovarian serous epithelial cancer from our institution. ADC histogram analysis was performed using FeAture Explorer software after outlining the whole lesion area on the ADC map. The ADC histogram parameter difference between subgroups was compared; the correlation between the quantitative parameters on MRI and Ki-67 expression was calculated for both groups. Results: The repeatability of ADC measurements across the two methods was good; the area method (ADCarea) had better performance in repeatability than the ROI method (ADCroi). The ADCroi, ADCarea, Ktrans, and Kep values significantly differed between the groups ($P < 0.05$). The histogram parameters (percent10, entropy, minimum, range and variance) and DCE parameter (Ktrans) were strongly correlated with Ki-67 expression ($P = 0.000$), while the conventional ADC measurements were not significantly correlated with Ki-67 expression ($P > 0.05$). Overall, Ktrans had the best diagnostic performance for discriminating type I with type II ovarian cancers (AUC = 0.826). Conclusion: In the present study, both diffusion-weighted imaging (DWI) and DCE MRI could help classify ovarian cancer patients with high accuracy. ADC histogram analysis could accurately reflect the proliferative capability of tumor cells to some extent.

Keywords: Ovarian epithelial cancer, magnetic resonance imaging, apparent coefficient value, diffusion-weighted imaging

Introduction

Ovarian cancer is a leading cause of gynecological malignancy-related death. The most common pathological subtype is ovarian epithelial cancer (OEC), which causes 75% of all ovarian cancer-related deaths [1]. As the most common subtype of ovarian malignancies, OEC also includes two subtypes: type I and type II [2]. Recent studies suggested that these two etiologies originate from various histologies coupled with different gene mutations. Type I OEC clinically develops slowly and has a relatively good prognosis [2-4]; however, type II OEC (high-grade serous cancer, HGSC) develops rapidly with a persistent chemotherapy-resistant response, and its prognosis is dismal. Accurate preoperative diagnosis can help clinicians design precise treatment strategies [5].

Magnetic resonance imaging (MRI) is a useful method for detecting ovarian masses [6-8]. MRI techniques such as diffusion-weighted imaging (DWI) could be used to differentiate

malignant from benign masses. The use of a quantitative index of the ADC value helps to assess the malignant potential of tumors [9]. Ovarian cancers always have lower ADC values than benign tumors with a poor prognosis. Histogram parameters are the most common radiomics signatures derived from imaging modalities [10-12]. ADC histogram analysis may reflect heterogeneity differences within tumors and help to determine the ovarian cancer subtypes [13, 14]. Dynamic contrast-enhanced magnetic resonance imaging (DCE-MRI), with multiple scanning circles at the target area, is another widely used technique that can help to determine the etiology of suspected masses. In a recent study, DCE-MRI histogram parameters were shown to predict the recurrence of HGSC [15]. For malignancies, the tumors always display both rapid enhancement and clearance, which is different from benign tumors that have homogeneously uniform enhancement after injection of contrast. However, limited studies have focused on comparing the performance of these two techniques in differentiating ovarian cancer subtypes, especially between type I and type II. The purpose of this study was to evaluate the diagnostic performance of tumor ADC histogram signatures on MRI in discriminating type I from type II lesions by comparing histogram analysis with DCE-MRI measurements and assessing the correlation between MRI parametric features and histological findings.

Material and methods

Patients

Our institutional review board (Gynecological and Obstetric Hospital, School of Medicine, Fudan University, China) approved this retrospective study, and the requirement for informed consent was waived for all participants. From January 1, 2019, to December 31, 2020, the data of patients with clinically suspected ovarian malignancies were retrieved from the picture archiving communication systems server of our institution. Female patients who were suspected of OEC and underwent a pelvic MRI scan before surgery were included in the study. The exclusion criteria were as follows: 1) gynecological malignancy history; 2) previous pelvic surgery/radiation therapy; 3) severe motion/movement artifacts; and 4) incomplete MRI data (patients who were claustrophobic or underwent MRI examination at other institutions) or final histological results. Ultimately, a total of 52 patients met the criteria, including 25 patients with type I ovarian tumors and 27 patients with type II ovarian tumors.

MRI acquisition and interpretation

MRI was performed using a 1.5-T system (Magnetom Avanto, Siemens) with a phased-array coil. The routine MRI protocols used for the assessment of pelvic masses included axial turbo spin-echo (TSE) T1-weighted imaging (T1WI), coronal TSE T2WI, and axial/sagittal TSE fat-saturated T2WI (FS T2WI). For axial images, the transverse plane was perpendicular to the long axis of the uterine body; for sagittal images, the longitudinal plane was parallel to the main body of the uterus. DWI was performed in the axial plane using an echo-planar imaging two-dimensional (EP2D) sequence and a parallel acquisition technique, with *b* values of 0, 100, and 800 s/mm^2. A DCE sequence was performed after the intravenous administration of 0.2 mmol/kg gadopentetate dimeglumine (Gd-DTPA, Magnevist; Bayer Schering) at a rate of 3.0 ml/s, followed by injection of 20 ml of normal saline to flush the tube. The scanning parameters were as follows: TR/TE = 5.6/2.38 ms, slice thickness = 4 mm; gap = 1.0 mm; matrix = 256 × 256; field of view = 280-340 mm, flip angle = 10°, and NEX = 1. A total of 30 phases of scans were obtained sequentially at 7-s intervals for 3 min 20 s. Every phase consists of 20 images.

All lesion interpretations on MR were performed by two experienced radiologists (both with more than 10 years of experience). The tumor maximum diameter (MD) and mass component were separately recorded for each patient. Two ADC measurement methods were applied and accomplished manually by two operators on a commercially available postprocess workstation. For the region of interest (ROI) measurement method, we placed the ROI-selecting tool into the center of the lesion with an average area of 180-220 mm^2 on the maximum solid component (or the center of the lesion in a purely cystic mass) on the ADC map (ADCroi). For the area measurement (ADCarea) method,

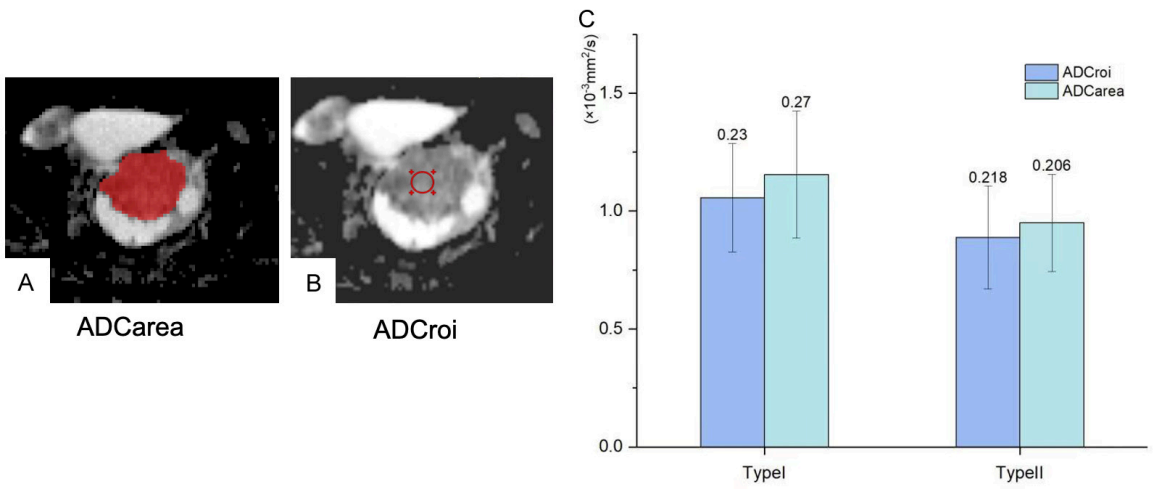

Figure 1. A 50-year-old woman with EC. The ADCarea (A) and ADCroi (B) methods showed the maximum lesion plane on the ADC map and the differences in the mean ADC values of the two methods across the two groups (C). ADC, Apparent Diffusion Coefficient.

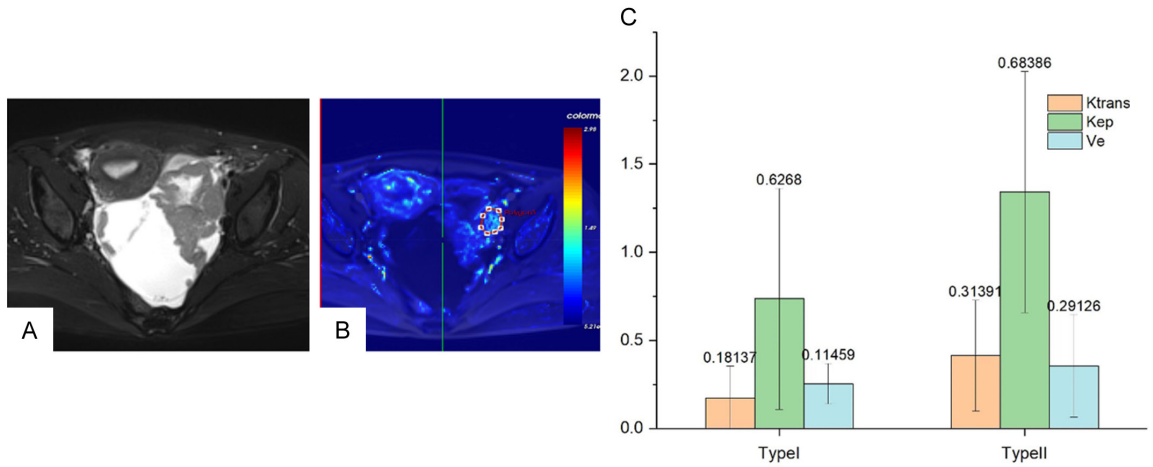

Figure 2. A 46-year-old woman with HGSC. The axial fat-saturation T2WI sequence (A), the corresponding dynamic perfusion map images (B), and the median value differences of three parameters across the two groups (C). HGSC, High-Grade Serious Cancer; ADC, Apparent Diffusion Coefficient; T2WI, T2 weighted imaging.

we outlined the whole lesion area on the maximum lesion plane on the ADC map (**Figure 1**).

DCE parameters were manually measured with Omni Kinetics software (Version V2.1.0. R, GE). In brief, after loading the total set of DCE images, we traced the vessels with a fully contrast-enhanced curve near the main tumor body (most is the iliac artery) to generate the Ktrans, Kep and Ve maps (**Figure 2**). Inter- and intraoperator consistency on both DWI and DCE MRI measurements were evaluated on 6 randomly selected patients with an interval of one month. The Ki-67 expression results were retrieved from the hospital information system for each patient. ADC histogram features were extracted from the ROI with PyRadiomics (http://pyradiomics.readthedocs.io/en/latest/index.html), including energy, total energy, entropy, minimum, 10th percentile, 90th percentile, maximum, mean, median, interquartile range, range, mean absolute deviation, robust mean absolute deviation, root mean squared, skewness, kurtosis, variance and uniformity [16].

Statistical analysis

All values are given as the mean ± standard deviation or median ± numerical range. An

Table 1. Demographic summaries of the selected samples

Group		Num	Age (mean ± sd)	*P* value	Ki-67 expression* (%)	*P* value
Type I		25		*P* = 0.072	30 (20, 60)	*P* = 0.205
	EC	7			20 (20, 60)	
	CCC	14			35 (28, 60)	
	LGSC	4			25 (6, 40)	
Type II	HGSC	27	54.6±9.4		50 (20, 65)	

EC, Endometrial Cancer; CCC, Clear Cell Cancer; LGSC, Low-Grade Serious Cancer; HGSC, High-Grade Serious Cancer; *median (lower quartile, upper quartile).

unpaired *t* test was performed if the continuous variables were normally distributed. The Mann-Whitney *U* test was used for nonnormally distributed data. Correlation analysis was used to analyze the association between MRI parameters and Ki-67 expression. The area under the receiver operating characteristic (ROC) curve (AUC) was calculated for various measurement parameters in differentiating the two histological types. The Bland-Altman test was used to evaluate intra/interoperator agreement in ADC measurements. The AUC was calculated for quantification. We used bootstrapping with 1000 estimates and applied a *t test* to acquire the 95% confidence interval (CI) of the AUC. The accuracy (ACC), sensitivity (SEN), specificity (SPE), positive predictive value (PPV), and negative predictive value (NPV) were also calculated to compare the performance of different methods. A *P* value of less than 0.05 indicated statistical significance. SPSS (SPSS Inc., version 13.0) and MedCalc (Version 19.1.7, MedCalc software) were used to perform all statistical analyses.

Results

Clinical and MRI characteristics

In this study, we included 52 patients comprising 14 patients with clear cell cancer (CCC), 7 patients with endometrial cancer (EC), 4 patients with low-grade serious cancer (LGSC) and 27 patients with HGSC. CCC, EC and LGSC were classified as type I ovarian cancer, and HGSC was classified as type II ovarian cancer. Thus, there were only two groups in our study, including 25 type I ovarian cancers and 27 type II ovarian cancers. The ages at onset among patients with type I tumors and type II tumors were 49.0±12.5 years and 54.6±9.4 years, respectively. There was no significant difference in age or Ki-67 expression between the two groups (**Table 1**).

Conventional ADC measurements and histogram analysis

The ADCroi and ADCarea values were significantly lower in patients with type II tumors than in those with type I tumors ($P < 0.05$, **Table 2**). When the cutoff value of ADCroi was 1.020×10^{-3} mm^2/s, it yielded an SEN of 76.0% and an SPE of 85.2% (AUC = 0.797, **Table 3**; **Figure 3**). The ADC histogram parameters and their performance in distinguishing type II tumors from type I tumors are listed in **Table 3**. Overall, the p10, p90, kurtosis, mean, median, minimum and range values significantly differed between the two groups (**Table 3**). The intraclass correlation coefficients of ADCroi and ADCarea were 0.876 and 0.952, respectively, and the interclass correlation coefficients were 0.732 and 0.779, respectively (**Table 4**; Supplementary Figures 1, 2).

Comparison between DCE and DWI MRI parameters in ovarian tumor categorization and tumor cell proliferation

Ktrans and Kep values were significantly greater in type II tumors than in type I tumors ($P < 0.05$); however, Ve values were similar in the type I and type II groups ($P > 0.05$, **Table 2**). The intraclass correlation coefficients of Ktrans, Kep, and Ve were 0.308, 0.760 and 0.721, respectively; the interclass correlation coefficients were 0.574, 0.343 and 0.276, respectively (**Table 4**). The correlation between DCE MRI parameters (Ktrans and Ve) and ADC histogram parameters (p10, entropy, minimum, range and variance) was observed. ADC histogram features achieved a better correlation with Ki-67 expression than the conventional ADC measurements (**Figure 4**).

Table 2. Quantitative measurements on DWI and DCE MRI in the selected samples

Group	Num	Maximum Diameter*	*P* value	DWI (mean ± std)				Dynamic enhanced MRI						
				ADCarea	*P* value	ADCroi	*p* value	Num	Ktrans*	*P* value	Kep	*P* value	Ve*	*P* value
Type I	25	12.5±2.8	*P* = 0.006	1155.2±269.7	*P* = 0.003	1057.1±229.6	*P* = 0.009	23	0.09 (0.05, 0.24)	*P* = 0.000	0.74±0.63	*P* = 0.001	0.232 (0.16, 0.36)	*P* = 0.57
EC	7	9.8±6.5		1073.2±261.5		979.9±214.9			0.05 (0.039, 0.11)		0.53±0.32		0.19 (0.07, 0.28)	
CCC	14	13.6±2.6		1238.4±176.8		1150.2±130.5			0.09 (0.055, 0.23)		0.63±0.49		0.23 (0.19, 0.39)	CCC
LGSC	4	10.2± 2.5		816.3±358.7		713.7±298.7			0.34 (0.097, 0.64)		1.40±1.01		0.34 (0.15, 0.43)	LGSC
Type II	27							22						
HGSC		8.2±3.4		950.4±206.1		888.2±218.0			0.288 (0.21, 0.58)		1.3422±0.68		0.244 (0.16, 0.51)	

DWI, Diffusion Weighted Imaging; DCE-MRI, Dynamic Contrast Enhanced MRI; EC, Endometrial Cancer; CCC, Clear Cell Cancer; LGSC, Low-Grade Serious Cancer; HGSC, High-Grade Serious Cancer; *median (lower quartile, upper quartile).

Table 3. ADC and histogram analysis in the selected samples and the corresponding significant difference at the statistical level

Parameters	Percent10	Percent90	Energy	Entropy	Kurtosis	Maximum	Mean	Median	Minimum	Range	Variance	ADCroi	ADCarea
Type 1	974.6±333.8	1520.3±408.1	3529446231.1±5733935273.8	4.0±0.6	4.3±2.1	2056.3±525.2	1236.5±365.3	1222.9±373.1	408.2±457.7	1648.1±656.9	54140.0±32979.9	1057.1±229.6	1073.2±261.5
Type 2	679.7±168.2	1266.5±306.6	4583648514.2±7158697097.0	4.1±0.5	5.8±2.7	2208.3±616.5	940.6±234.6	895. 1±238.3	100.37±196.9	2107.9±660.6	66874.5±29328.1	888.2±218.0	950.4±206.1
P value	0.000	0.008	0.513	0.442	0.015	0.289	0.000	0.000	0.002	0.007	0.114	0.009	0.003
AUC*	0.784	0.691	0.403	0.432	0.283	0.391	0.745	0.765	0.692	0.283	0.354	0.797	0.796

ADC, Apparent Diffusion Coefficient; AUC, Area Under the Curve; *means taking type II as the positive group.

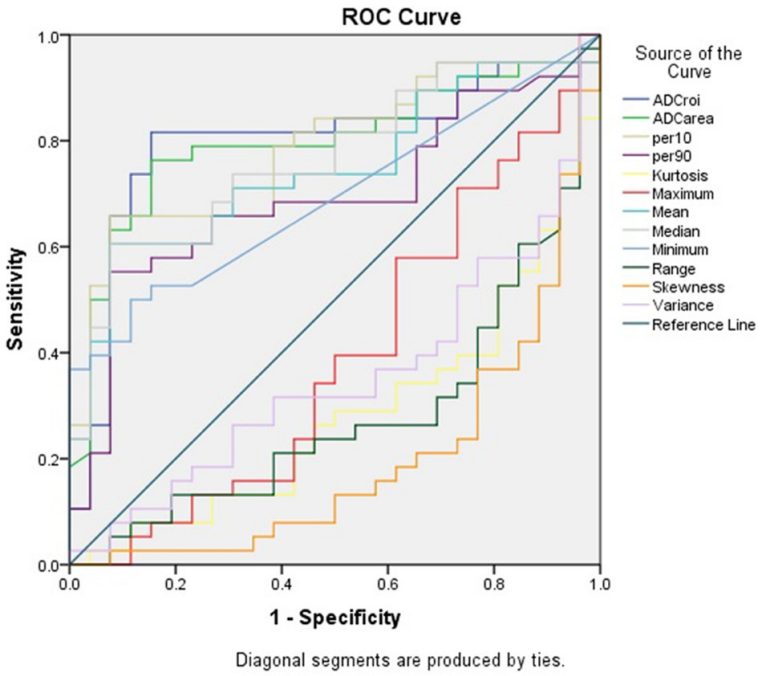

Figure 3. Diagnostic performance of conventional ADC, ADC histogram and DCE-MRI parameters in the differentiation between type I and type II tumors. ADC, Apparent Diffusion Coefficient; DCE-MRI, Dynamic Contrast Enhanced MRI; ROC, Receiver Operating Characteristic.

Discussion

In this study, both ADC- and DCE-derived parameters had high performance in categorizing OEC subtypes. The DCE parameter Ktrans and some ADC histogram features were significantly correlated with tumor invasive ability compared with the conventional ADC measurement.

Ovarian cancer is a highly non-homogeneous tumor including a wide spectrum of etiologies with various imaging characteristics and post-treatment outcomes [17]. On conventional MRI, OEC mostly presents as a large cystic mass with thick, irregular septa and nodular or solid components enhancing on postcontrast images [18]. The advantage of MRI is that it can help to discriminate malignancies from benign conditions preoperatively based on the morphological changes on various protocols of MR images. Type II cancer (mostly HGSC) is the most lethal type of tumor, accounting for more than 90% of all ovarian cancers. How to preoperatively judge this type still poses a challenge for both radiologists and clinicians. DCE-MRI, as a functional imaging method, can reflect blood flow kinetics to some extent by rapidly and repeatedly scanning the targeted area after contrast injection. Numerous studies have also reported that the indices derived from DCE sequences help to determine the etiology of complex adnexal masses [19, 20]. Our findings also corroborated this point. The difference between this study and the previous one is that we found that the repeatability of the DCE MRI parameters was obviously lower than that of the ADC index. Furthermore, by using this technique, we focused on classifying the selected samples into two subtypes, which was also different from other similar studies. The major limitation is that the selected reference image map is heavily vessel signal dependent. Thus far, the postprocess software for dealing with DCE MRI data is not commercially used in clinical units, mostly for scientific research.

Diffusion weighted imaging is another functional modality method reflecting water molecular brown movement in tissues. The ADC value is a quantitative index indicating the restriction degree of water molecular freedom movement. In one article, the authors reported that the ADC value of tumors in ovarian cancer was more negatively correlated with Ki-67 index expression than in other cancers (lung cancer, prostate cancer, colon cancer, etc.). The Ki-67 index is a proliferative parameter of tumor cells, meaning that more invasive tumors have higher Ki-67 expression [21]. Our previous studies reported that the ADC value helps clinicians differentiate primary adnexal malignancies from benignities, which have much higher ADC values than cancer tissue [22]. However, studies focusing on OEC subtype differentiation are still limited [23]. In this study, by using two measurement methods, the mean ADC value in type II tumors was much lower than that in type I tumors. A possible reason may be that the cellular atypia of HGSC under

Table 4. Inter- and intraoperator measurements summaries in the 6 randomly selected samples

Parameters		ADCarea	ADCroi	Ktrans	Kep	Ve
Inter	Operator 1	1174±308	1082±123	0.5143±0.3025	1.0261±0.6803	0.4428±0.3541
	Operator 2	989±260	1114±159	0.6317±0.6409	1.5285±0.9274	0.4091±0.3121
	ICC	0.779	0.732	0.574	0.343	0.276
Intra	First-round	1159±208	1058±251	0.3603±0.2604	0.9173±0.7499	0.0790±0.0933
	Second-round	1204±225	946±255	0.4781±0.5730	1.1889±1.2401	0.1117±0.1180
	ICC	0.952	0.876	0.308	0.760	0.721

ADC, Apparent Diffusion Coefficient; ICC, Intraclass Coefficient.

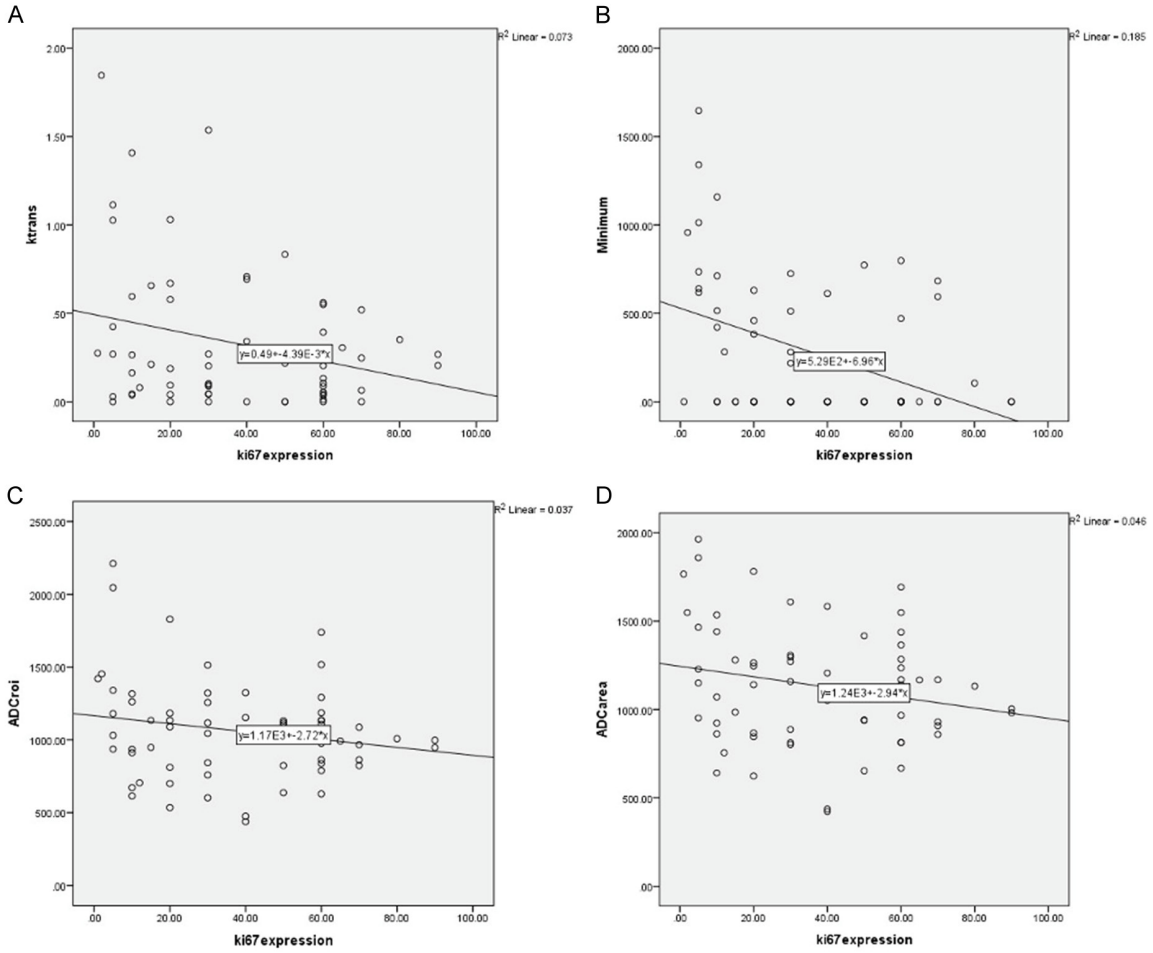

Figure 4. Scatter plots of the correlations between Ktrans (A), the minimum ADC value (B), ADCroi (C) and minimum ADCarea (D) and ki67 expression. ADC, Apparent Diffusion Coefficient.

microscopy is more obvious than that seen in type I tumors [24].

Given the consistency of the two measuring methods, both methods had better agreement for both for intra- and interoperator measurements [25]. In contrast to the whole lesion outlining the ADC area, the ROI method only placed the circle into the center of the tumor solid components. This ADC measurement method in ovarian cancer is relatively independent of lesion size and the operator's subjective impression. Mukuda N et al. reported that the ROI shape influenced ADC values and the optimal cutoff ADC value for differentiating benign from malignant ovarian tumors [26]. In another

study, the authors declared that the five small ROIs method in endometrial carcinoma had the best interclass correlation coefficient in ADC measurements [27]. ADC histogram analysis has been proven helpful in gynecological tumor categorization and prognosis prediction [11, 12, 28]. In this study, ADC histogram features achieved a better correlation with Ki-67 expression than the conventional ADC measurements. A possible reason could be that histogram features may be more reflective of the heterogeneity of the tumor body [11].

Our study has several limitations. First, there were limited numbers of samples of OEC subtypes in this study, and a larger sample size will facilitate the interpretation of the conclusions. Second, we only compared the ADC values with the Ki-67 expression in the microscopic findings. More correlations between the ADC value and the cell morphological changes could be helpful in determining the true mechanism of the ADC value differences between the two etiologies. Third, in this study, 1.5T MRI equipment was applied. 3.0T MRI may improve image resolution with a high signal-to-noise ratio and fast scanning protocols. Future studies will help clarify the differences between the two MRI units.

Conclusions

In summary, both DWI and DCE MRI could help to classify ovarian cancer patients with high accuracy. ADC histogram analysis could accurately reflect the proliferative capability of tumor cells to some extent.

Disclosure of conflict of interest

None.

Abbreviations

ADC, Apparent Diffusion Coefficient; OEC, Ovarian Epithelial Cancer; MRI, Magnetic Resonance Imaging; LGSC, Low-Grade Serous ovarian Cancer; HGSC, High-Grade Serous ovarian Cancer; 3D, Three-Dimensional; DWI, Diffusion-Weighted Imaging; ROI, Region Of Interest; MD, Maximum Diameter; T1WI, T1-Weighted Imaging; T2WI, T2-Weighted Imaging; ROC curve, Receiver Operating Characteristic curve.

Address correspondence to: Yuantao Liu, Department of Gynecology, Obstetrics and Gynecology Hospital of Fudan University, Shanghai, P. R. China. Tel: +86-13761299475; E-mail: lesleyanimal@hotmail.com; He Zhang, Department of Radiology, Obstetrics and Gynecology Hospital, Fudan University, Shanghai, P. R. China. Tel: +86-13917826540; E-mail: dr.zhanghe@yahoo.com

References

[1] Bowtell DD, Böhm S, Ahmed AA, Aspuria PJ, Bast RC Jr, Beral V, Berek JS, Birrer MJ, Blagden S, Bookman MA, Brenton JD, Chiappinelli KB, Martins FC, Coukos G, Drapkin R, Edmondson R, Fotopoulou C, Gabra H, Galon J, Gourley C, Heong V, Huntsman DG, Iwanicki M, Karlan BY, Kaye A, Lengyel E, Levine DA, Lu KH, McNeish IA, Menon U, Narod SA, Nelson BH, Nephew KP, Pharoah P, Powell DJ Jr, Ramos P, Romero IL, Scott CL, Sood AK, Stronach EA and Balkwill FR. Rethinking ovarian cancer II: reducing mortality from high-grade serous ovarian cancer. Nat Rev Cancer 2015; 15: 668-679.

[2] Goulding EA, Simcock B, McLachlan J, van der Griend R and Sykes P. Low-grade serous ovarian carcinoma: a comprehensive literature review. Aust N Z J Obstet Gynaecol 2020; 60: 27-33.

[3] Slomovitz B, Gourley C, Carey MS, Malpica A, Shih IM, Huntsman D, Fader AN, Grisham RN, Schlumbrecht M, Sun CC, Ludemann J, Cooney GA, Coleman R, Sood AK, Mahdi H, Wong KK, Covens A, O'Malley DM, Lecuru F, Cobb LP, Caputo TA, May T, Huang M, Siemon J, Fernández ML, Ray-Coquard I and Gershenson DM. Low-grade serous ovarian cancer: state of the science. Gynecol Oncol 2020; 156: 715-725.

[4] Pauly N, Ehmann S, Ricciardi E, Ataseven B, Bommert M, Heitz F, Prader S, Schneider S, du Bois A, Harter P and Baert T. Low-grade serous tumors: are we making progress? Curr Oncol Rep 2020; 22: 8.

[5] Prahm KP, Karlsen MA, Høgdall E, Scheller NM, Lundvall L, Nedergaard L, Christensen IJ and Høgdall C. The prognostic value of dividing epithelial ovarian cancer into type I and type II tumors based on pathologic characteristics. Gynecol Oncol 2015; 136: 205-211.

[6] Khan SR, Arshad M, Wallitt K, Stewart V, Bharwani N and Barwick TD. What's new in imaging for gynecologic cancer? Curr Oncol Rep 2017; 19: 85.

[7] Medeiros LR, Freitas LB, Rosa DD, Silva FR, Silva LS, Birtencourt LT, Edelweiss MI and Rosa MI. Accuracy of magnetic resonance imaging in ovarian tumor: a systematic quantita-

tive review. Am J Obstet Gynecol 2011; 204: 67, e1-10.
[8] Thomassin-Naggara I, Poncelet E, Jalaguier-Coudray A, Guerra A, Fournier LS, Stojanovic S, Millet I, Bharwani N, Juhan V, Cunha TM, Masselli G, Balleyguier C, Malhaire C, Perrot NF, Sadowski EA, Bazot M, Taourel P, Porcher R, Darai E, Reinhold C and Rockall AG. Ovarian-adnexal reporting data system magnetic resonance imaging (O-RADS MRI) score for risk stratification of sonographically indeterminate adnexal masses. JAMA Netw Open 2020; 3: e1919896.
[9] Surov A, Meyer HJ and Wienke A. Associations between apparent diffusion coefficient (ADC) and KI 67 in different tumors: a meta-analysis. Part 1: ADCmean. Oncotarget 2017; 8: 75434-75444.
[10] Gerges L, Popiolek D and Rosenkrantz AB. Explorative investigation of whole-lesion histogram MRI metrics for differentiating uterine leiomyomas and leiomyosarcomas. AJR Am J Roentgenol 2018; 210: 1172-1177.
[11] Schob S, Meyer HJ, Pazaitis N, Schramm D, Bremicker K, Exner M, Höhn AK, Garnov N and Surov A. ADC histogram analysis of cervical cancer aids detecting lymphatic metastases-a preliminary study. Mol Imaging Biol 2017; 19: 953-962.
[12] Thapa D, Wang P, Wu G, Wang X and Sun Q. A histogram analysis of diffusion and perfusion features of cervical cancer based on intravoxel incoherent motion magnetic resonance imaging. Magn Reson Imaging 2019; 55: 103-111.
[13] Guan Y, Shi H, Chen Y, Liu S, Li W, Jiang Z, Wang H, He J, Zhou Z and Ge Y. Whole-lesion histogram analysis of apparent diffusion coefficient for the assessment of cervical cancer. J Comput Assist Tomogr 2016; 40: 212-217.
[14] Li HM, Zhang R, Gu WY, Zhao SH, Lu N, Zhang GF, Peng WJ and Qiang JW. Whole solid tumour volume histogram analysis of the apparent diffusion coefficient for differentiating high-grade from low-grade serous ovarian carcinoma: correlation with Ki-67 proliferation status. Clin Radiol 2019; 74: 918-925.
[15] Li HM, Tang W, Feng F, Zhao SH, Gu WY, Zhang GF and Qiang JW. Whole solid tumor volume histogram parameters for predicting the recurrence in patients with epithelial ovarian carcinoma: a feasibility study on quantitative DCE-MRI. Acta Radiol 2020; 61: 1266-1276.
[16] van Griethuysen JJM, Fedorov A, Parmar C, Hosny A, Aucoin N, Narayan V, Beets-Tan RGH, Fillion-Robin JC, Pieper S and Aerts HJWL. Computational radiomics system to decode the radiographic phenotype. Cancer Res 2017; 77: e104-e107.
[17] Lalwani N, Prasad SR, Vikram R, Shanbhogue AK, Huettner PC and Fasih N. Histologic, molecular, and cytogenetic features of ovarian cancers: implications for diagnosis and treatment. Radiographics 2011; 31: 625-646.
[18] Rajkotia K, Veeramani M and Macura KJ. Magnetic resonance imaging of adnexal masses. Top Magn Reson Imaging 2006; 17: 379-397.
[19] Thomassin-Naggara I, Balvay D, Aubert E, Daraï E, Rouzier R, Cuenod CA and Bazot M. Quantitative dynamic contrast-enhanced MR imaging analysis of complex adnexal masses: a preliminary study. Eur Radiol 2012; 22: 738-745.
[20] Li HM, Qiang JW, Xia GL, Zhao SH, Ma FH, Cai SQ, Feng F and Fu AY. MRI for differentiating ovarian endometrioid adenocarcinoma from high-grade serous adenocarcinoma. J Ovarian Res 2015; 8: 26.
[21] Korkolopoulou P, Vassilopoulos I, Konstantinidou AE, Zorzos H, Patsouris E, Agapitos E and Davaris P. The combined evaluation of p27Kip1 and Ki-67 expression provides independent information on overall survival of ovarian carcinoma patients. Gynecol Oncol 2002; 85: 404-414.
[22] Zhang H, Zhang GF, He ZY, Li ZY and Zhang GX. Prospective evaluation of 3T MRI findings for primary adnexal lesions and comparison with the final histological diagnosis. Arch Gynecol Obstet 2014; 289: 357-364.
[23] Liu D, Zhang L, Indima N, Peng K, Li Q, Hua T and Tang G. CT and MRI findings of type I and type II epithelial ovarian cancer. Eur J Radiol 2017; 90: 225-233.
[24] Hatano Y, Hatano K, Tamada M, Morishige KI, Tomita H, Yanai H and Hara A. A comprehensive review of ovarian serous carcinoma. Adv Anat Pathol 2019; 26: 329-339.
[25] Lindgren A, Anttila M, Rautiainen S, Arponen O, Kivelä A, Mäkinen P, Härmä K, Hämäläinen K, Kosma VM, Ylä-Herttuala S, Vanninen R and Sallinen H. Primary and metastatic ovarian cancer: characterization by 3.0T diffusion-weighted MRI. Eur Radiol 2017; 27: 4002-4012.
[26] Mukuda N, Fujii S, Inoue C, Fukunaga T, Tanabe Y, Itamochi H and Ogawa T. Apparent diffusion coefficient (ADC) measurement in ovarian tumor: effect of region-of-interest methods on ADC values and diagnostic ability. J Magn Reson Imaging 2016; 43: 720-725.
[27] Inoue C, Fujii S, Kaneda S, Fukunaga T, Kaminou T, Kigawa J, Harada T and Ogawa T. Apparent diffusion coefficient (ADC) measurement in endometrial carcinoma: effect of region of interest methods on ADC values. J Magn Reson Imaging 2014; 40: 157-161.
[28] Onodera K, Hatakenaka M, Yama N, Onodera M, Saito T, Kwee TC and Takahara T. Repeatability analysis of ADC histogram metrics of the uterus. Acta Radiol 2019; 60: 526-534.

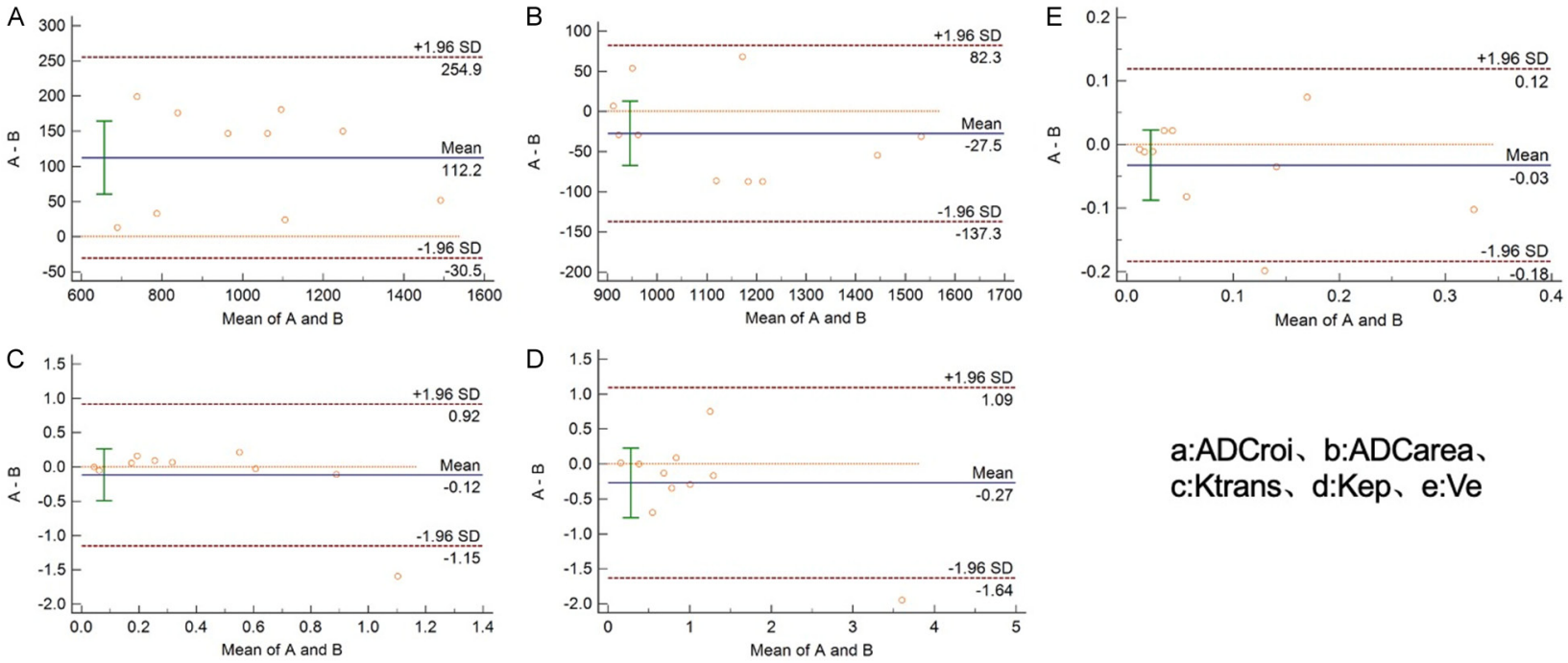

Supplementary Figure 1. The scatter plots of the correlation between ADCroi and minimum ADCarea and ki67 expression. ADC, Apparent Diffusion Coefficient.

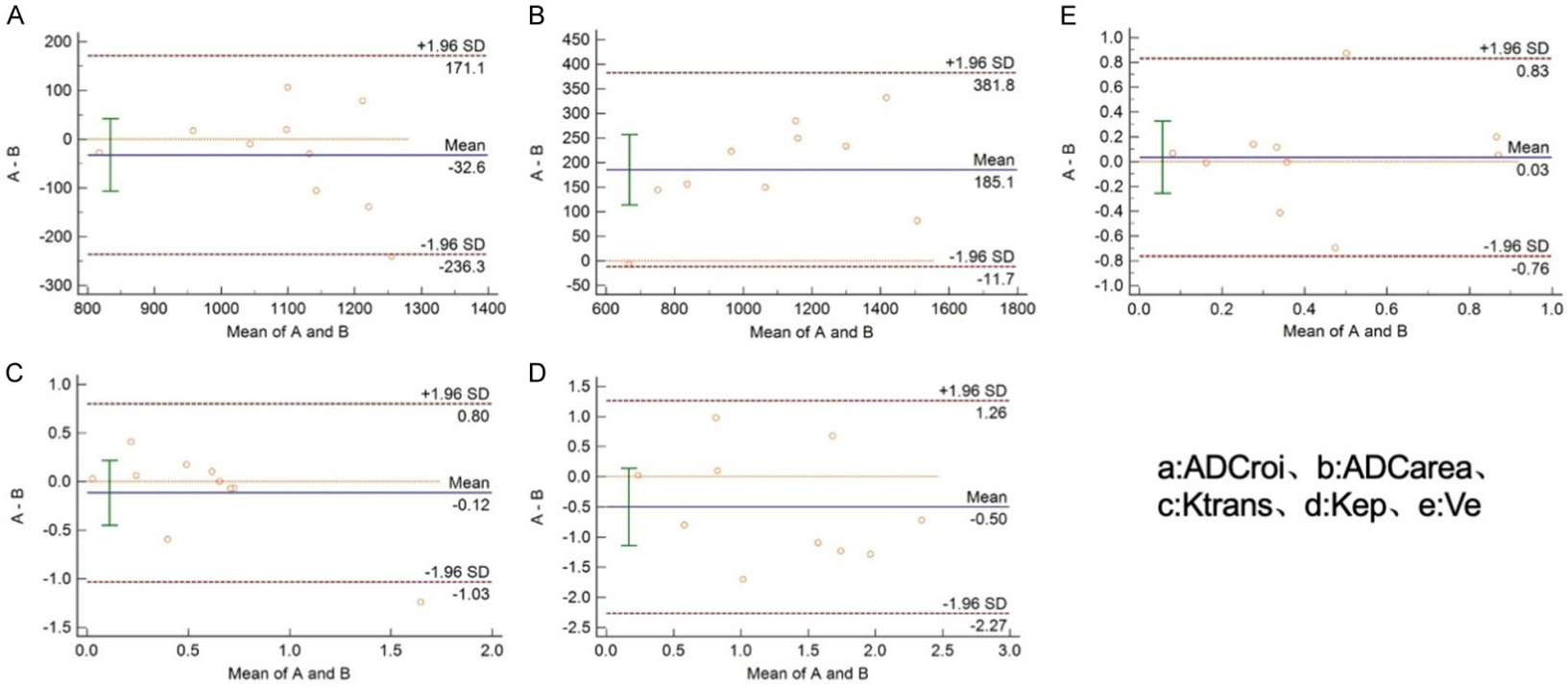

Supplementary Figure 2. The Bland plots of intraoperator's measurement consistency in five parameters. ADC, Apparent Diffusion Coefficient.